Accepted Manuscript

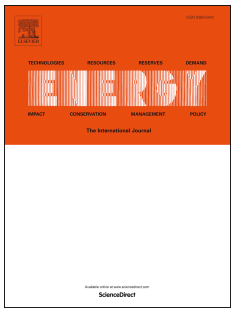

Performance of the domestic micro ORC equipped with the shell-and-tube condenser with minichannels

Jan Wajs, Dariusz Mikielewicz, Blanka Jakubowska

PII: S0360-5442(18)31018-1

DOI: 10.1016/j.energy.2018.05.174

Reference: EGY 13009

To appear in: *Energy*

Received Date: 12 February 2018

Revised Date: 24 May 2018

Accepted Date: 26 May 2018

Please cite this article as: Wajs J, Mikielewicz D, Jakubowska B, Performance of the domestic micro ORC equipped with the shell-and-tube condenser with minichannels, *Energy* (2018), doi: 10.1016/j.energy.2018.05.174.

Performance of the domestic micro ORC equipped with the shell-and-tube condenser with minichannels

Jan WAJS *, Dariusz MIKIELEWICZ, Blanka JAKUBOWSKA

Department of Energy and Industrial Apparatus, Gdansk University of Technology,
Narutowicza 11/12, 80-233 Gdansk, Poland

jan.wajs@pg.edu.pl, dariusz.mikielewicz@pg.edu.pl, blanka.jakubowska@pg.edu.pl

* Corresponding author. Email: jan.wajs@pg.edu.pl

HIGHLIGHTS:

- Shell-and-tube condenser with minichannels is considered.
- Sizing calculations of condenser dedicated to micro-CHP ORC unit are performed.
- In-house model of pressure drop and condensation is applied to heat exchanger sizing.
- Experimental validation of the prototype shell-and-tube heat exchanger is carried out.

Abstract: In this paper, the original compact shell-and-tube heat exchanger with circular minichannels of in-house design and manufacturing is presented as the condenser for the domestic micro heat and power plant investigations as well as other future technical applications. The heat exchanger is equipped with turbulizing baffles inside the shell. The shell itself is made of a tubular sleeve having an inner diameter of 0.067 m and the length of 0.38 m. The tube bundle constitutes of 103 pipes arranged hexagonally with the active length equal to 0.31 m. The tubes inner diameter equals to 0.002 m and the wall thickness is 0.001 m. The calculations of the heat transfer coefficient for the condensation in the flow of the ethanol as a working fluid was done by means of several methods, among others the one developed in-house. That model accounts for the non-adiabatic effects in the convective heat transfer coefficient. The experimental validation of the prototype construction was accomplished. During the tests the condenser was cooled by water with ethanol as a working fluid. The obtained results are in a good consistency with the in-house model predictions.

Keywords: Shell-and-tube heat exchanger, Micro-CHP, Minichannels, Condensation, Theory application, Experimental analysis

Nomenclature

A - surface (m^2)
B - blowing parameter (-)
Bo - boiling number (-)
c - specific heat (kJ/(kgK))
C - coefficient in Eq. (1) (-)
Con - constraint number (1) (-)
d_i - tube inner diameter (m)
D_h - hydraulic diameter (m)
f - friction factor (-)
g - gravity (m/s^2)
G - mass flux ($kg/(m^2s)$)

Ga - Galileo number
$H(\varepsilon)$ - function of void fraction in Huang et al. model (-)
L - distance (m)
$\dot{m}$ - mass flow rate (kg/s)
p - pressure (Pa)
P - empirical correction factor (-)
P_h - phase change number (-)
q - heat flux (W/m^2)
$\dot{Q}$ - rate of heat (W)
Pr - Prandtl number (-)
R_{2f} - two-phase multiplier (-)
Re - Reynolds number (-)
T - temperature (°C)
u - velocity (m/s)
x - vapour quality (-)
X_{tt} - Martinelli parameter

Greek letters:

α - heat transfer coefficient (W/(m^{2}K))
Δ - difference value
η - efficiency
λ - thermal conductivity (W/(mK))
μ - viscosity (Pa s)
ρ - density (kg/m^3)
σ - surface tension (N/m)

Subscripts:

E - ethanol
el - electrical
exp - experiment
lE - liquid ethanol
vE - vapour of ethanol
f - frictional
i - inner
in - inlet
out - outlet
Pb - pool boiling
T - turbine
w - water
1*f* - single-phase

2f - two-phase
2f_b - two-phase – boiling
2f_c - two-phase – condensation

1. Introduction

European Union energy policy places an emphasis on the energy efficiency improvement, energy sector security and the need for energy production diversification in the member countries. To fulfill these requirements the particular tasks were defined. They are realized through the rationalization of classical energy technologies (based on the combustion of fossil fuels such as coal and gas) and searching for new directions of cogeneration/trigeneration energy production in the distributed systems (often based on renewable energy resources). The role of the distributed systems is to assist the centralized system operation. The current approach to the electric energy production is a kind of prosumer one, in which the system user can be the energy consumer and also its seller to the power grid. In accordance with the micro-CHP potential analysis of the European market [1] the distributed systems (micro CHP) can be divided in three groups namely: systems with internal combustion, systems with external combustion and fuel cells (Fig. 1). The social awareness and then public interest in such systems are constantly increasing and their expected sale in selected EU countries in 2030 is listed in Table 1 [1].

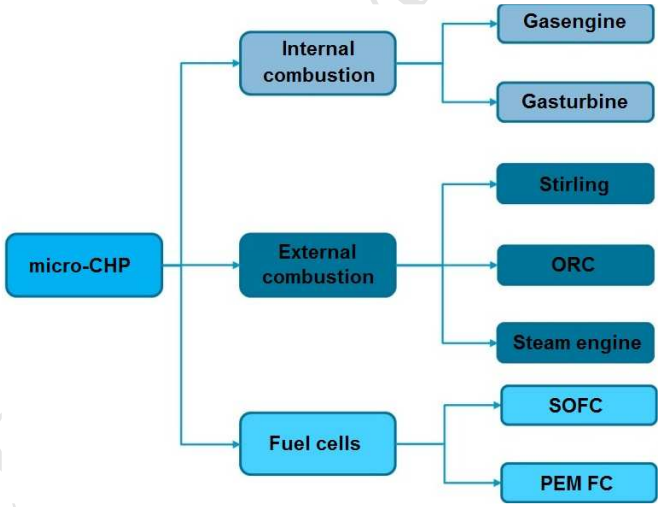

Fig. 1. Micro-CHP technologies [1].

Table 1
Expected sale of micro-CHP systems in selected EU countries in 2030 [1].

country	thousand units/year	country	thousand units/year
United Kingdom	763	Ireland	35
Italy	742	Austria	27
Netherlands	303	Poland	27
France	289	Czech Republic	26
Spain	276	Hungary	22
Germany	215	Portugal	22
Belgium	89	Romania	18

Considering the mentioned in Fig. 1 technologies and their development, the ORC system seems to be the closest to the commercialization stage from a variety of micro-CHP domestic units. Research works regarding this topic are conducted in many research centers around the world, just to mention a few [2-4]. However, it should be pointed out that the practical realization of the organic Rankine cycle (ORC) in a micro-scale (the electrical power production below 10 kW_e) is still a kind of technical challenge. Such a unit must be equipped with small size turbine or expansion machine as well as highly efficient and compact heat exchangers (evaporator and condenser, sometimes also the regenerator), as the overall footprint of the installation should not be too large. This is the reason why novel constructions of recuperators or enhancement mechanisms are sought for. In the literature, a description of many active, passive or combined techniques of heat transfer rate augmentation can be found. One of the common ways of increasing the heat transfer coefficient during the two-phase flow convective heat transfer is to reduce the channel dimensions [5, 6]. In such a case often laminar flows are encountered. The intensification of heat transfer in the case of circular channels with laminar flows can be based on different kinds of inserts [7]. A lot of methods are applied to increase the thermal performance of heat transfer devices such as treated surfaces [8], porous surfaces [9], rough surfaces [10], coiled tubes [11] or surface tension devices [12].

Researchers have been developing a prototype of the cogenerative boiler for household applications for some time now. It should be mentioned that the complete system of such kind was not reported so far. A demonstration prototype micro-CHP unit based on ORC technology was developed [13]. The system consists of the ORC module (with ethanol as a working fluid) coupled with the commercial gas boiler through the loop with the heating oil. The boiler is commercially available on the market and used in many houses. The idea of such a system is to produce electricity for household demand or for selling it to electric grid – in such a situation the system user will became the prosumer. Investigations show that the boiler with a thermal power of 25 kW was able to provide the saturated/superheated vapour of ethanol at proper conditions needed in the ORC system and it can be utilized as a heat source in the domestic micro-CHP. The tested system could produce electricity in the amount of 1 kW_e [14].

In the paper, a prototype of the compact shell-and-tube condenser with circular minichannels of in-house design and manufacturing is presented as the unit for the domestic micro CHP investigations as well as other future technical applications. The calculations of the convective heat transfer coefficient in the tubes for the prototype of the condenser were accomplished based on the semi-empirical model, developed in-house, which accounts additionally for the non-adiabatic effects. The results of the heat transfer calculations were compared with the predictions by other correlations available in the literature [16-21]. An experimental validation of the prototype construction was also done – the tests were provided using the authors own micro-CHP installation mentioned above. During this study the prototype construction served as the condenser cooled by water with ethanol as a working

fluid.

2. Sizing of the condenser

Based on the first author's own experience with compact heat exchanger technologies [10,22,23], the novel shell-and-tube heat exchanger with minichannels dedicated to the ORC module integrated with domestic gas boiler was designed. The construction with one shell pass and one tube pass (cross-counterflow mode of operation) was chosen. At the beginning of the design process, it was assumed that the tube bundle would consist of smooth straight pipes of inner/outer diameter equal to 0.002 m / 0.004 m, respectively, while the shell would be constructed of 0.067 m inner diameter cylinder. Design activities were supported with the theoretical modeling of single and two-phase convection heat transfer and hydraulic resistance. The input parameters used in the calculations were defined in the basis of prior own experimental analysis regarding the micro CHP technology with ethanol as working fluid [13]. These parameters were also confirmed with the design of the prototype micro turbogenerator. The values of applied in a calculation procedure parameters are listed in Table 2. The essential physical properties of water and ethanol were taken from Refprop 9.0 [24]. In Table 3 the selected properties of ethanol at saturation temperature 45 °C are presented. The theoretical considerations are described below. All calculations were performed with Engineering Equation Solver (EES) [25].

Table 2

The input data used in a calculation procedure.

Parameter	Value
Rate of heat, (kW)	20
Condensation temperature of ethanol, (°C)	45
Ethanol mass flow rate, (kg/s)	0.022
Vapour quality,	$1 \rightarrow 0$
Water inlet temperature, (°C)	13
Water outlet temperature, (°C)	35

Table 3

The selected properties of ethanol at 45 °C [24].

Property	Value
Heat of vaporation, (kJ/kg)	898.8
Density of saturated liquid, (kg/m^3)	768.1
Density of dry saturated vapour, (kg/m^3)	0.4078
Dynamic viscosity of liquid, (Pa·s)	$0.757 \cdot 10^{-3}$
Dynamic viscosity of vapour, (Pa·s)	$9.079 \cdot 10^{-6}$
Thermal conductivity of liquid, (W/(m·K))	0.1597
Thermal conductivity of vapour, (W/(m·K))	0.018
Specific heat of liquid, (kJ/(kg·K))	2.75
Specific heat of vapour, (kJ/(kg·K))	1.601

2.1. Thermal-hydraulic calculations

The algorithm of thermal-hydraulic calculations of the condensation heat transfer was executed based on the iterative method. As it was mentioned before, the in-house semi-empirical correlation [15] was used to describe the flow condensation in minichannels. This correlation accounts the non-adiabatic effects in the determination of the convective heat transfer coefficient, which modifies the friction pressure drop term and subsequently the heat transfer coefficient.

In accordance with the general correlation [15] the heat transfer coefficient in the two-phase flow (boiling or condensation) is described by the following equation:

$$\frac{\alpha_{2f}}{\alpha_{1f}} = \sqrt{R_{2f}{}^{n} + \frac{C}{1+P}\left(\frac{\alpha_{Pb}}{\alpha_{1f}}\right)^2} \tag{1}$$

where: α_{1f} – single-phase convection heat transfer coefficient of ethanol,

R_{2f} – two-phase flow multiplier, defined as:

$$R_{2f} = \frac{\Delta p_{2f}}{\Delta p_{1f}} \tag{2}$$

P – empirical correction factor,

α_{Pb} – pool boiling heat transfer coefficient,

C – coefficient: $C = 1$ (flow boiling), $C = 0$ (flow condensation),

n – exponent: $n = 0.76$ (turbulent), $n = 2$ (laminar).

The empirical correction factor P in Eq. (1) is needed in the case of flow boiling and is described as:

$$P = 2.53 \cdot 10^{-3} \cdot \mathrm{Re}_{lE}{}^{1.17} \cdot \mathrm{Bo}^{0.6} \cdot (R_{2f\_b} - 1)^{-0.65} \tag{3}$$

where Bo is the boiling number, Re_{lE} is the Reynolds number for the liquid ethanol and the R_{2f_b} – multiplier for the flow boiling.

The method described by Eq. (1) has a general applicability and can be used in the determination of heat transfer in both the flow boiling and flow condensation in the conventional size channels as well as the minichannels. The main assumption in the modeling

process of the flow boiling/flow condensation was related to the fact that the fluid in the flow boiling / flow condensation was treated as an homogeneous with the properties of the two-phase mixture. Moreover, it is modeled as a sum of two contributions leading to the total energy dissipation in the flow, namely the energy dissipation due to the shearing flow without the bubbles and the dissipation resulting from the bubble generation/collapse [26]. During flow condensation the heat transfer coefficient (α_{2f_c}) can be calculated from Eq. (1) at the assumption that C=0. This results in the omission of the part of the model connected with the bubble generation, which is not present during condensation. In this case the equation (1) reduces to the form:

$$\frac{\alpha_{2f}}{\alpha_{lE}} = R_{2f\_c} \tag{4}$$

where R_{2f_c} is a two-phase flow multiplier appropriately formulated for condensation.

The equation describing the two-phase flow multiplier takes into account the non adiabatic impact for the two-phase multiplier during flow condensation. Depending on the structure of the flow it can be described as:

$$R_{2f\_c} = \begin{cases} R \cdot (1 + \dfrac{B}{2}) & \textit{for annular flow} \\ R\sqrt{1 + \left(\dfrac{8 \cdot \alpha_{Pb} \cdot d_i}{\lambda_{lE} \cdot \mathrm{Re}_{lE} \cdot \mathrm{Pr}_{lE} \cdot f_r \cdot R} \right)^2} & \textit{for other flow structures} \end{cases} \tag{5}$$

where B – blowing parameter,

d_i – inner diameter of tube in the bundle,

λ_{lE} – coefficient of liquid ethanol thermal conductivity,

f_r – friction factor,

R – two-phase multiplier.

In Eq. (5) there is no specification of which the two-phase flow multiplier model should be applied. That issue is dependent upon the type of considered fluid. In the present study leading to the development of the minichannel heat exchanger the Müller – Steinhagen and Heck correlation [27] modified by D. Mikielewicz and J. Mikielewicz [15] to account for the surface tension forces for applicability in the small diameter channels, which reads:

$$R = \left[1 + 2\left(\frac{1}{f_1} - 1 \right) \cdot x \cdot \mathrm{Con}^m \right] \cdot (1 - x)^{1/3} + \frac{1}{f_{1z}} \cdot x^3 \tag{6}$$

In Eq. (6), in the case of the conventional diameter of the channels the value of the exponent m=0 whereas in the case of the small diameter channels m=-1, f_1 and f_{1z} are the functions which take into account the flow regime; f_1 is defined as a ratio of pressure drop in the single phase liquid to the pressure drop in the single phase vapour, whereas f_{1z} is defined as a ratio of heat transfer coefficient in the single phase flow of the vapour to the single phase heat transfer coefficient for the liquid.

In Eq. (6) Con is the constraint number, which takes into account the surface tension. Surface tension plays a dominant role in the creation of two-phase flow structures in small

diameter channels [28]. The constraint number is determined accordingly to the formula:

$$\mathrm{Con} = \frac{\left[\dfrac{\sigma}{g(\rho_{lE} - \rho_{vE})}\right]^{0.5}}{d_i} \tag{7}$$

where: σ is the surface tension and g – gravity. For the laminar flow functions f_1 and f_{1z} can be expressed by the following formulas:

$$f_1 = \frac{\mu_{lE}}{\mu_{vlE}} \cdot \frac{\rho_{vE}}{\rho_{lE}} \tag{8}$$

$$f_{1z} = \frac{\mu_{vE}}{\mu_{lE}} \cdot \frac{c_{lE}}{c_{vE}} \cdot \left(\frac{\lambda_{lE}}{\lambda_{vE}}\right)^{1.5} \tag{9}$$

After substituting the liquid and vapour ethanol physical properties to Eqs. (8) and (9) the following values were obtained $f_1 = 0.0427$ and $f_{1z} = 0.5093$.

The blowing parameter which is a part of Eq. (5), and is defined as:

$$B = \frac{2 \cdot q \cdot \dfrac{\rho_{lE}}{\rho_{vE}}}{f_r \cdot G(s-1) \cdot h_{lv}} \tag{10}$$

where s is the slip ratio, which can be determined from the Zivi formula [29]:

$$s = \sqrt[3]{\frac{\rho_{lE}}{\rho_{vE}}} \tag{11}$$

The distribution of the two-phase flow multiplier (R_{2f_c}) dependent on the quality (x) is presented in Fig. 2. The obtained values of the heat transfer coefficient during the condensation of the ethanol in the minichannel (α_{2f_c}) are summarized in Fig. 3.

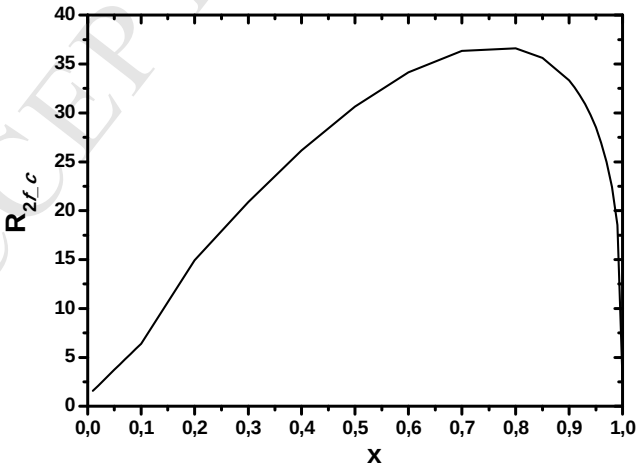

Fig. 2. Two-phase multiplier distribution versus quality of the ethanol; $G_E = 68$ kg/(m^{2}s), d_i=0.002 m.

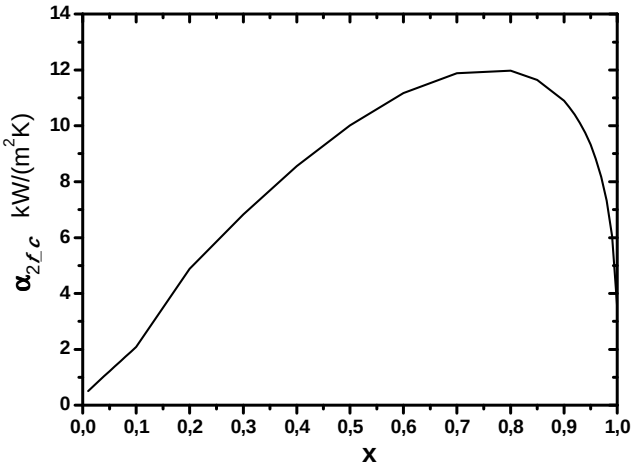

Fig. 3. Distribution of the heat transfer coefficient during the flow condensation of the ethanol G_E = 68 kg/(m^{2}s), d_i=0.002 m.

In the heat transfer process modeling, on the water side (heated fluid inside condenser), the correlation for the cross-flow across a bank of tubes was applied. For the staggered tube rows in the bundle, the Nusselt number can be defined as [30]:

$$\mathrm{Nu}_w = c\left(\frac{a}{b}\right)^r (\mathrm{Re}_w)^m (\mathrm{Pr}_w)^n \left(\frac{\mathrm{Pr}_w}{\mathrm{Pr}_{w\_w}}\right)^{0.25} \tag{12}$$

where the coefficients c, r, m, and n in the range of the Reynolds number values $10^3 < \mathrm{Re}_w < 2\cdot 10^5$ are equal to c = 0.35, r = 0.2, m = 0.6, n = 0.36, respectively. The coefficients a and b are defined in the basis of geometrical dimensions (the notation is consistent with Fig. 4):

$$a = \frac{y_1}{d_o}, \qquad b = \frac{y_2}{d_o} \tag{13}$$

The heat transfer coefficient was determined by the transformation of the Nusselt number definition:

$$\alpha_w = \frac{\lambda_w \cdot \mathrm{Nu}_w}{D_h} \tag{14}$$

where λ is the thermal conductivity of the water and D_h is the hydraulic diameter defined as:

$$D_h = \frac{D^2 - n \cdot d_o^2}{D + n \cdot d_o} \tag{15}$$

In Eq. (15) n is the number of pipes in the bundle.

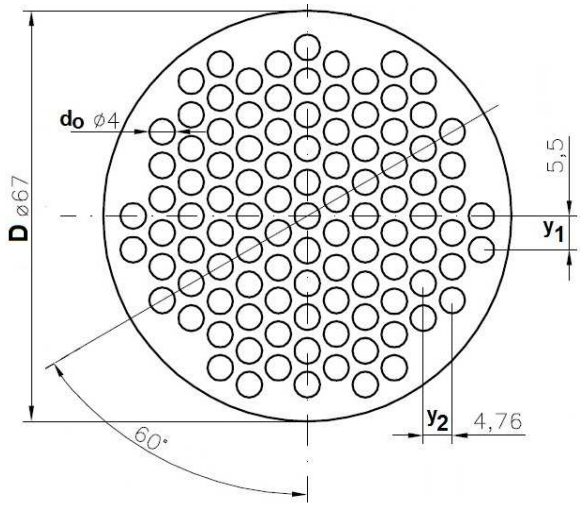

Fig. 4. Scheme of staggered tube rows in the bundle.

The pressure drop on the shell side is an effect of the cooling water inflow dynamics and the presences of the baffles, which ensure the turbulent flow. It depends on the number of pipes in the bundle, and the number of baffles. The total pressure drop was determined using the Kern method [31]:

$$\Delta p_{shell} = \frac{f_T \cdot G_s{}^2 \cdot (N_B + 1) \cdot D}{2 \cdot \rho_w \cdot D_h \cdot \left(\frac{\mu_w}{\mu_{w\_w}} \right)^{0.14}} \tag{16}$$

where: f_T – friction factor,

G_s – mass flux of water,

N_B – number of baffles,

D – inner shell diameter,

D_h – hydraulic diameter of the shell.

The shell side friction coefficient includes the inlet and outlet losses and can be calculated from the formula [32]:

$$f_T = \exp\left(0.576 - 0.19 \cdot \ln(\mathrm{Re}_w)\right) + C_f \tag{17}$$

where C_f is the friction corrector factor. It is dependent on the tube pitch and tube diameter ratio and the Reynolds number.

The pressure drop on the ethanol side (the cooled fluid inside the condenser) is the result of the phase change (condensation). Furthermore, the pressure drop inside the tubes is caused by friction during the two-phase flow and the acceleration of the fluid caused by the phase change. The change of hydrostatic pressure in the analyzed condenser is negligible due to the small length of the tubes in the bundle. Therefore, the tube side total pressure drop was calculated by knowing the two-phase multiplier and the single-phase flow pressure drop:

$$\Delta p_{2f} = R \cdot \Delta p_{1f} \tag{18}$$

The two-phase multiplier was calculated with Eq. (6). The pressure drop of the liquid ethanol single-phase flow in a single tube was described by the following relation:

$$\Delta p_{1f} = f_r \cdot \frac{L}{d_i} \cdot 0.5 \cdot \rho_{lE} \cdot u_{lE}^2 \tag{19}$$

where f_r is the friction factor (defined for the laminar flow as f_r=64/Re$_E$), L is the length of the single tube, d_i – the inner diameter of the tube in the bundle and u_{lE} – the mean ethanol velocity inside the tube.

The pressure resilience calculations of the presented heat exchanger construction were done in accordance with the relevant standards for the pressure equipment provided by the Office of Technical Inspection [33]. It was verified if the assumed wall thickness of the particular components (shell, tube sheet, bottom, and connections) were sufficient to withstand the working stresses. For this purpose various pressure and temperature values up to the maximal pressure of 3 MPa and temperature of 200 °C were applied to the system. In all of the analyzed cases the working stresses were lower than the admissible ones.

2.2. Flow condensation heat transfer coefficient – comparison with the correlations

The analysis of the ethanol condensation heat transfer was also done with the application of the models available in the literature. Since modeling of two phase heat transfer is very complex and causes higher level of uncertainties only the well-known correlations were used. The models regarding the annular flow in the convectional channels and minichannels were chosen. The calculations allowed the comparison with the semi-empirical Mikielewicz correlation [15] applied in the designing process of the presented heat exchanger prototype. The correlations due to Akers et al. [16], Shah [17], Cavallini and Zecchin [18], Boyko and Kruzhilin [18], Huang et al. [19], Park et al. [20] and Kim and Mudawar [21] have been selected for comparisons.

A pioneering work of flow condensation modeling done by Akers et al. [16], is valid for the most commonly found flow structure, namely the annular flow. The model was developed on the basis of experiments with propane, methanol and refrigerant R12.

Empirical correlation due to Shah [17] is one of the most general and widely used for calculations of heat transfer coefficients in flow condensation. It has been developed on the basis of the experimental data accomplished for water, R11, R12, R22, R113, methanol, ethanol, toluene and trichloroethylene flowing in vertical, horizontal and inclined tubes (d_i = 0.007-0.040 m). The formulation of this model was concluded that in the case of nucleate boiling absence, which is the case for condensation, the heat transfer coefficient should be close to the one for the annular flow structure.

Another model used for comparative purposes is the semi-empirical model proposed by Cavallini and Zecchin (cited in [18]). It was elaborated based on the experimental data collected for the condensation of a variety of organic refrigerants (such as R11, R12, R22, R113) in horizontal and vertical pipes.

The Boyko and Kruzhilin correlation (cited in [18]) is also applied in the condensation of flow annular structure. It was developed on the basis of the experimental data accomplished

for steam and R22.

Among the correlations recommended for minichannels is the correlation due to Huang et al. [19]. It came from the experimental investigations of a mixture of refrigerant R410A and oil (concentration up to 5%). Tests were conducted inside the horizontal tube with inner diameter of 0.0016 and 0.00418 m.

In the case of Park et al. approach [20] the model was proposed in accordance with the flow condensation experimental study of refrigerants R134a, R236ea and R1234ze in vertically aligned minichannels. The hydraulic diameter of the rectangular cross-section was 0.00145 m. In this model a geometrical relation between respective Nusselt's numbers was assumed, namely the Nusselt number in the forced convective condensation and gravity controlled convection condensation.

A universal approach to the condensation heat transfer for mini- and microchannels modeling was proposed by Kim and Mudawar [21]. The authors collected the abundant experimental database, for the purpose of which the results were collected from various research centers and it consisted of 17 working fluids in the channels of hydraulic diameter in the range 0.000424-0.00622 m.

Table 4 provides a summary of the selected correlations recommended for the mini- and microchannels, whereas in Fig. 5 the results of the ethanol condensation heat transfer coefficient calculations are presented. Ultimately, the results obtained with Huang et al. [19] correlation were not shown in Fig. 5, due to the discrepancy reaching even several hundred percent in comparison with the other correlations. In the authors' opinion the reason of such a difference comes from the origin of this correlation, which was derived for the mixture of organic fluid and oil.

Table 4

Selected correlations describing the condensation heat transfer coefficient.

Author(s)	Equation	Remarks
Akers et al. (1959)	$\alpha_{2f\_c} = 0.026 \frac{\lambda_l}{d} \mathrm{Pr}_l^{1/3} \left[\frac{G(1-x)}{\mu_l} \right]^{0.8} \left[\frac{x}{(1-x)} \left(\frac{\rho_l}{\rho_g} \right)^{0.5} + 1 \right]$	Fluids: R12, methanol, propane
Boyko and Kruzhilin (1967)	$\alpha_{2f\_c} = \alpha_l \left[1 + x \left(\frac{\rho_l}{\rho_g} - 1 \right) \right]^{0.5}$, $\alpha_l = 0.021 \,\mathrm{Re}_l^{0.8} \,\mathrm{Pr}_l^{0.43} \frac{\lambda_l}{d_i}$	Fluids: steam, R22, 1500< Re <15000
Cavallini and Zecchin (1971)	$\alpha_{2f\_c} = \frac{\lambda}{d_i} 0.05 \,\mathrm{Re}_e^{0.8} \,\mathrm{Pr}^{0.33}$, $R_e = \mathrm{Re}_v \left(\frac{\rho_l}{\rho_v} \right)^{0.5} \left(\frac{\mu_v}{\mu_l} \right) + \mathrm{Re}_l$	Fluids: R12, R12, R21, R22, R113, R114, $\mathrm{Re}_l > 1.2 \cdot 10^3$, d_i = 8 mm
Shah (1979)	$\alpha_{2f\_c} = \alpha_l \left[(1-x)^{0.8} + \frac{3.8 x^{0.76} (1-x)^{0.04}}{(p/p_{kr})^{0.38}} \right]$, $\alpha_l = 0.023 \,\mathrm{Re}_l^{0.8} \,\mathrm{Pr}_l^{0.4} \frac{\lambda_l}{d_i}$	Fluids: water, R11, R12, R22, R113, methanol, ethanol, benzene, toluene, trichloroethylene, Re > 3000, d_i = 7-40 mm,
Huang et al. (2010)	$\alpha_{2f\_c} = \frac{\lambda}{d_i} \sqrt{Nu_F^{\,2} + Nu_B^{\,2}}$, $Nu_F = 0.0152 \left(\frac{R_{2f}}{X_{tt}} \right) \mathrm{Re}_l^{0.77} \left(-0.33 + 0.83 \,\mathrm{Pr}_l^{0.8} \right)$, $Nu_B = 0.725 \cdot H(\varepsilon) \cdot \left(\frac{Ga_l \,\mathrm{Pr}_l}{P_h} \right)^{0.25}$, $P_h = \frac{c_{pl} (T_{sat} - T_{wall,i})}{h_{lv}}$	Fluids: R410A-oil mixture, d_i = 1.6 and 4.18 mm
Park et al. (2011)	$\alpha_{2f\_c} = \frac{\lambda}{d_h} \sqrt{Nu_F^{\,2} + Nu_B^{\,2}}$, $Nu_F = 0.0055 \,\mathrm{Pr}_l^{1.37} \left(\frac{R_{2f}}{X_{tt}} \right) \mathrm{Re}_l^{0.7}$, $Nu_B = 0.746 \left(1 - e^{-0.85\sqrt{Bo}} \right) \cdot H(\varepsilon) \cdot \left(\frac{Ga_l \,\mathrm{Pr}_l}{P_h} \right)^{0.25}$	Fluids: R134a, R236ea, R1234ze, d_h = 1.45 mm
Kim and Mudawar (2013)	$\alpha_{2f\_c} = \frac{\lambda_l}{d_h} 0.048 \,\mathrm{Re}_l^{0.69} \,\mathrm{Pr}_l^{0.34} \frac{R_{2f}}{X_{tt}}$	data for 17 fluids, d_h = 0.424-6.22 mm

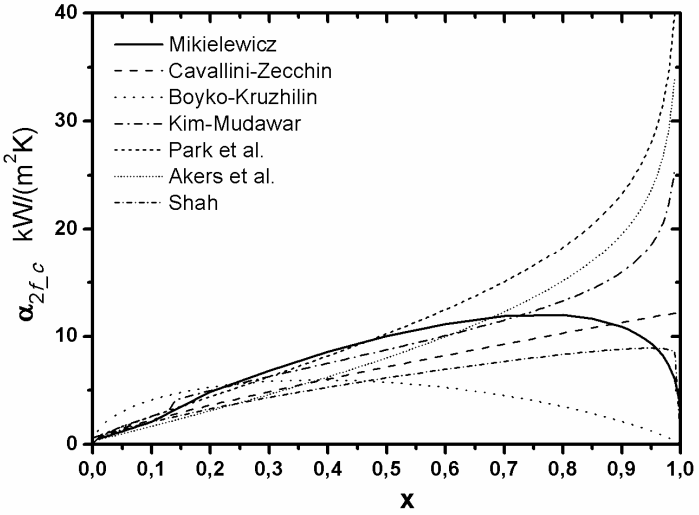

Fig. 5. Results of the ethanol condensation heat transfer coefficient calculations.

As can be seen from Fig. 5 there is a significant discrepancy between the predictions obtained using different correlations from the literature. It ought to be borne in mind that some of the correlations, namely due to Akers et al., Boyko and Kruzhilin, Cavallini and Zecchin as well as due to Shah were developed for condensation in channels featuring the diameter greater than 6 mm, which these days is regarded as conventional channels. The correlations due to Park et al., Kim and Mudawar as well as the one due to one of the present authors are applicable to minichannels, i.e. diameters smaller than 3 mm. A correct qualitative behaviour is represented by only three correlations, namely due to Boyko and Kruzhilin, Shah and Mikielewicz. In these correlations the asymptotic behavior of the heat transfer distribution is correct, however, quantitative differences are present. A similar distribution is presented by the correlations due to Shah and Mikielewicz. Some of the literature studies indicate that the model due to Shah is a recommended tool in the calculation of heat transfer in flow condensation, so in the present case it was assumed as a reference of heat transfer calculations. In the considered example however the challenge is to predict accurately the condensation of the fluid, for which the applicable correlations were not validated. That is the major reason for the discrepancy between the models. That is not present in the model described by Eq. (4) which is independent of the type of fluid. Many tests confirmed a good performance of the model in predicting the heat transfer deficiency coefficient in condensation. The model was also tested for the flow boiling of the ethanol, showing a good consistency. Therefore, the subsequent sizing calculations of the heat exchanger were carried out based on the predictions of the Shah's model and Eq. (4).

2.3. Shell-and-tube condenser with minichannels

As it was mentioned earlier, the tube bundle was assembled with the tubes which inner diameter equal to 0.002 m, thickness of the wall equal to 0.001 m and active length of 0.31 m. To ensure the diversion of the flow across the bundle to obtain higher values of the heat transfer coefficient due to turbulization the baffles were installed inside the shell. They also support the tubes for structural rigidity, preventing tube vibrations and deflections. The baffles covered 80% of the shell cross-section [34] and were made of 0.001 m thick steel plate and were equally spaced arranged along the tubes bundle. All heat exchanger components were made of stainless austenitic chrome-nickel steel 316L according to AISI standard. The tubes were connected with the tube sheets using the TIG welding technology same as the other joints. The shell was made of 0.073 m diameter pipe, while the heat exchanger end faces and bundle tube sheets were made of 0.005 m thick steel plate. The heat transfer area was equal to 0.4 m^2, heat exchanger entire length was 0.37 m and its weight was 5.4 kg.

The presented heat exchanger was designed as a condenser operating in the micro CHP system. The ethanol was chosen as the working medium and its condensation was occurring inside the tubes bundle. Water was used as the cooling medium, therefore it was flowing through the shell, watering the tubes. For the calculation purpose the following assumption

was made: ethanol entered the heat exchanger as the dry saturated vapour and left it as the saturated liquid.

The axonometric views and photography of the minichannel shell-and-tube condenser are presented in Fig. 6. Its geometric details are listed in Table 5.

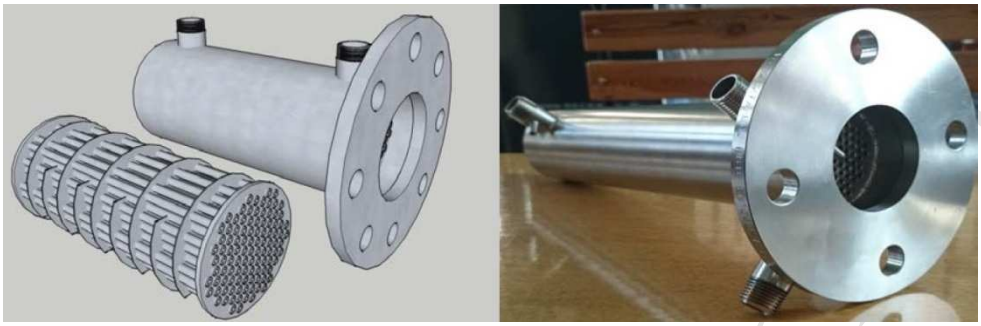

Fig. 6. Original shell-and-tube condenser with bundle made of minitubes.

Table 5

The characteristic dimensions of the condenser.

Parameter	Value
Inner diameter of shell	67 mm
Number of pipes in a bundle	103
Active length of tube in the tube bundle	310 mm
Inner diameter of tube	2 mm
Wall thickness of tube	1 mm
Heat exchange surface	0.4 m^2
Number of turbulizing baffles	9

3. Experimental

The designed shell-and-tube condenser was implemented in the micro-CHP unit. The laboratory stand (schematically shown in Fig. 7) consists of a gas boiler as an autonomous source of heat (1), oil pump (2), oil flowmeter (3), evaporator of ORC module (4), turbine and generator inside common casing (5-6), condenser (7), ethanol pump (8), ethanol flowmeter (9), cooling water flowmeter (10), safety equipment (11,12), throttle valve (13). The general view of the facility is presented in Fig. 8, while the view of the turbine combined with the original condenser through the compensator is shown in Fig. 9.

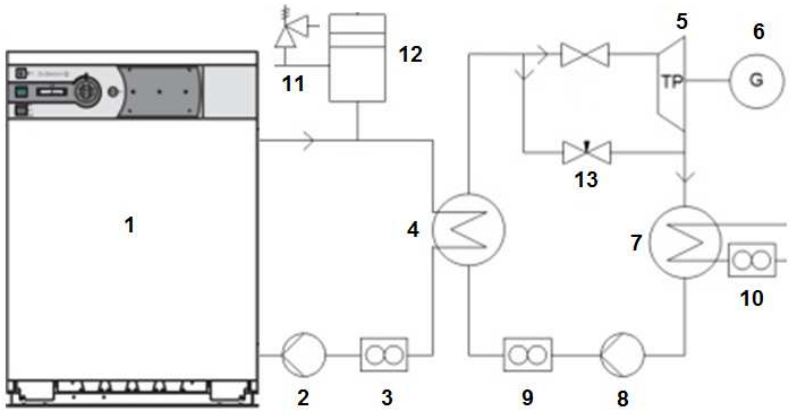

Fig. 7. Schematic of the domestic micro ORC system.

The domestic gas boiler (De Dietrich company) delivers heat to the thermal oil Mobiltherm 603. Oil is an intermediate heat transfer medium circulating in a closed loop between the boiler and evaporator of the vapour cycle with working fluid dehydrated ethyl alcohol. Oil circulation in the loop was ensured by the Wilo ST20/6 pump with a maximum volume flow rate of 3.5 m^3/h and a maximum head of 6 m. A vane flow meter was used to measure the volumetric flow of oil. The circulation of the ethanol in a closed loop of the ORC module was provided by a hermetic gear pump (Tuthill, model TXS2.6) with magnetic coupling of a nominal volume flow rate of 0.4 m^3/h at a differential pressure of 10.3 bar. The adjustment of the pump's efficiency was possible by changing the frequency. A Danfoss Coriolis-type mass flow meter MASS 2100 working with MASS 6000 19" IP20 signal converter was used to measure the liquid flow of the ethanol. The working fluid passing through the evaporator received heat from the thermal oil and evaporated to reach the state of the vapour with the applied appropriate heat flux. Saturated/superheated vapour was directed to the ORC turbine, where it expanded and then flowed to the condenser. The turbine was connected with the condenser by means of a flexible compensator providing the damping in the system. During the facility start-up phase the turbine was always bypassed by the throttling valve to obtain the required vapour parameters. After that the valve was closed. As it was mentioned earlier, the condenser was cooled by water. The water volumetric flow rate was measured by the Magflo (MAG 3100) electromagnetic flowmeter. After the condensation process, the liquid ethanol was turned back to the reservoir.

The key element in the installation is the axial microturbine [35] designed and constructed for the needs of the prototype micro-CHP, with an ethanol vapour as the working fluid. The generator is set on the turbine shaft, directly behind its low-pressure section – the turbine and generator assembly therefore have a common casing. The microturbine is equipped with a single supersonic turbine stage (the Mach number at the outlet of the steering rack is 2.4, the design rotor speed is 36000 rpm). The design alcohol mass output is 25 g/s, its vapour pressure at the turbine inlet is 7 bar, and the vapour pressure after expansion in the turbine is 1 bar. The turbine's bearings are lubricated by the ethanol vapours.

Fig. 8. General view of the micro-CHP ORC unit.

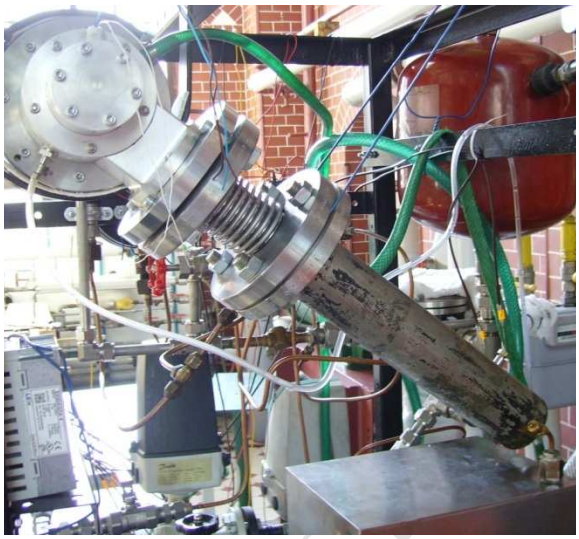

Fig. 9. View of the turbine combined with the novel shell-and-tube condenser through the compensator.

During the experiments the pressure was measured using the calibrated Bourdon pressure gauge, programmable pressure meters WW-11N and TRAFAG 8253 transducers (with accuracy of 0.15% of the whole scale). The temperature in the characteristic places of the circuit was measured by the T-type thermocouples with accuracy at the level of ±0.3 K. Such a level of thermocouples accuracy was obtained due to an individual sensor calibration procedure done by the system of very high accuracy. The thermocouples were connected with the CROPICO 3001 acquisition system, which had an internal reference temperature stabilizer. The results of the uncertainty analysis are presented in Table 6.

Table 6
Uncertainty of individual measurements.

Parameter	Operating range	Uncertainty
mass flow rate of ethanol (g/s)	15-20	±0.1%
mass flow rate of water (g/s)	150-220	±0.5%
temperature (°C)	10-150	±0.3°C
pressure (MPa)	0.36-0.6	±0.15%

All the tests were carried out in steady state conditions. Generally, during the experiments the boiler could produce the superheated vapour of the ethanol under the pressure 0.36–0.6 MPa and at the temperature up to 143°C. The mass flow rate of the ethanol was in the range from 15 to 20 g/s. The temperature of the cooling water at the inlet to the condenser was about 13°C. However, only the results of the particular measurement series are presented here. They corresponded with the values used in the theoretical considerations, therefore were taken to validate the thermal effectiveness of the in-house designed and constructed condenser. These results referred to the ethanol mass flow rate equal to 20 g/s, ethanol vapour quality of about 1 at the inlet to condenser and also the cooling water temperature being in the

range 13-35°C. On the basis of the measurement results the following values have been determined in the course of the experiments: the rate of heat received by the working medium (ethanol) in the evaporator ($\dot{Q}_{in}$), the rate of heat gained by the water in the condenser ($\dot{Q}_{out}$), the generation of electric power (N_{el}), micro-CHP electric efficiency (η_{el}), maximum efficiency, i.e. Carnot cycle efficiency in the min/max working temperature (η_C). The results of the measurements and calculations are summarized in Table 7. This table additionally features: the mass flow rates of ethanol ($\dot{m}_E$), the temperature and pressure of the ethanol at the turbine's inlet (T_{T_in}, P_{T_in}), the quality of the ethanol vapour at the condenser's inlet (x_{E_in}), the temperature of the ethanol subcooled liquid at the condenser's outlet (T_{E_out}), the mass flow rate of the cooling water ($\dot{m}_w$) and its temperature at the inlet ($T_{w,in}$) and outlet of the condenser ($T_{w,out}$).

Table 7

Performance of the micro-CHP unit with novel minichannels shell-and-tube condenser.

$\dot{Q}_{in}$	N_{el}	η_{el}	η_c	P_{T_in}	T_{T_in}	*condenser*							
						$\dot{m}_E$	P_{E_in}	x_{E_in}	$T_{E,out}$	$\dot{m}_w$	$T_{w,in}$	$T_{w,out}$	$\dot{Q}_{out}$
kW	kW	%	%	MPa	°C	g/s	MPa	–	°C	g/s	°C	°C	kW
21.26	0.66	6.65	22.53	0.573	130.4	20	0.159	0.98	22.6	218	13.7	35.2	19.63
21.29	0.71	6.10	20.66	0.529	129.6	20	0.153	0.99	33.0	206	13.2	35.4	19.19
21.48	0.76	6.40	23.54	0.604	143.2	19	0.156	– *	23.2	210	13.5	35.0	18.84

* superheated vapour ($\Delta t_{superheat}$ = 4.7 K)

For the mentioned above condenser conditions, the generation of electrical power up to 0.76 kW was obtained. It corresponded with the micro-CHP electrical efficiency in the range 6.1% – 6.7%. It is very good performance in comparison with the data gathered in [2], which exhibited the electrical efficiency below 5% for the generated electrical power about 1kW in the ORC system equipped with turbine.

4. Summary

The novel design and manufacture of the shell-and-tube condenser with minichannels was presented. Its thermal and hydraulic characteristics were calculated in the basis of several theoretical models from the literature as well as the in-house model. Significant discrepancy between correlations was found.

The in-house model together with the model due to Shah were used to determine the heat transfer coefficient during condensation inside the tubes.

The comparison between the considered correlations and the in-house mode showed the good consistency and predictability of the in-house model.

Experimental validation of the prototype construction was also done – the tests were provided using own micro-CHP installation with domestic gas boiler. In the course of the studies it was demonstrated that this installation ensured the thermal parameters of the vapour

suitable for a prototype micro-turbine and the generation of 760 W electric power. At the moment the reached electrical efficiency was at the level of about 6.7%, which was higher than the reported data in the very last literature overviews in the range up to 1kW of generated electric power. The obtained performance of the in-house micro-CHP system is very promising and demonstrates its potential.

References

[1] Cogeneration Observatory and Dissemination Europe (CODE2). Micro-CHP potential analysis European level report, http://www.code2-project.eu/wp-content/uploads/D2.5-2014-12-micro-CHP-potential-analysis_final.pdf; 2014 [accessed 9 February 2018].

[2] Landelle A, Tauveron N, Haberschill P, et al. Organic Rankine cycle design and performance comparison based on experimental database. Appl Energy 2017;204:1172–1187. DOI: 10.1016/j.apenergy.2017.04.012

[3] Ibarra M, Rovira A, Padilla, DCA, Blanco J. Performance of a 5 kWe Organic Rankine Cycle at part-load operation. Appl Energy 2014;120:147–158. DOI: 10.1016/j.apenergy.2014.01.057

[4] Borsukiewicz-Gozdur A. Experimental investigation of R227ea applied as working fluid in the ORC power plant with hermetic turbogenerator. Appl Therm Eng 2013;56:126–133. DOI: 10.1016/j.applthermaleng.2013.03.039

[5] Karayiannis TG, Mahmoud MM. Flow boiling in microchannels: fundamentals and applications. Appl Therm Eng 2017;115:1372–1397. DOI: 10.1016/j.applthermaleng.2016.08.063

[6] Garimella S. Condensation in minichannels and microchannels, chapter 6. In: Kandlikar SG et al., editors. Heat transfer and fluid flow in minichannels, NewYork: Elsevier; 2006.

[7] Mikielewicz D, Klugmann M, Wajs J. Flow boiling intensification in minichannels by means of mechanical flow turbulising inserts. Int J Therm Sci 2013;65:79–91. DOI: 10.1016/j.ijthermalsci.2012.10.002

[8] Piasecka M, Strąk K, Maciejewska B, Grabas B. A study of the flow boiling heat transfer in a minichannel for a heated wall with surface texture produced by vibration-assisted laser machining. Journal of Physics Conference Series 2016;745(3): 032123. DOI: 10.1088/1742-6596/745/3/032123

[9] Furberg R, Palm B, Li S, Toprak M, Muhammed M. The use of a nano- and microporous surface layer to enhance boiling in a plate heat exchanger. J Heat Trans-T ASME 2009;131(10): 101010. DOI: 10.1115/1.3180702

[10] Wajs J, Mikielewicz D. Influence of metallic porous microlayer on pressure drop and heat transfer of stainless steel plate heat exchanger. Appl Therm Eng 2016;93: 1337–1346. DOI: 10.1016/j.applthermaleng.2015.08.101

[11] Liu X, Xu X, Liu C, et al. Heat transfer deterioration in helically coiled heat exchangers in trans-critical CO_2 Rankine cycles. Energy 2018;147:1–14. DOI: 10.1016/j.energy.2017.12.163

[12] Attinger D, Frankiewicz C, Betz AR, et al. Surface engineering for phase change heat transfer: a review. MRS Energy Sustain 2014;1:E4. DOI: 10.1557/mre.2014.9

[13] Mikielewicz D, Wajs J, Mikielewicz J. Gas boiler as a heat source for a domestic micro-CHP. Journal of Power Technologies 2014;94:317–322.

[14] Wajs J, Mikielewicz D, Bajor M, Kneba Z. Experimental investigation of domestic

micro-CHP based on the gas boiler fitted with ORC module. Archives of Thermodynamics 2016;37(3):79–93. DOI: 10.1515/aoter-2016-0021

[15] Mikielewicz D, Mikielewicz J. A common method for calculation of flow boiling and flow condensation heat transfer coefficients in minichannels with account of nonadiabatic effects. Heat Transfer Eng 2011;32(13-14):1173–1181. DOI: 10.1080/01457632.2011.562728

[16] Akers WW, Deans HA, Crosser OK. Condensing Heat Transfer within Horizontal Tubes. Chem Eng Prog S Ser 1959;55(29):171–176.

[17] Shah MM. A general correlation for heat transfer during film condensation inside pipes. Int J Heat Mass Tran 1979;22:547–556.

[18] Sánta R. The analysis of two-phase condensation heat transfer models based on the comparison of the boundary condition. Acta Polytech Hung 2012;9(6):167–180.

[19] Huang X, Ding G, Hu H, et al. Influence of oil on flow condensation heat transfer of R410A inside 4.18 mm and 1.6 mm inner diameter horizontal smooth tubes. Int J Refrig 2010;33:158–169. DOI: 10.1016/j.ijrefrig.2009.09.008

[20] Park JE, Vakili-Farahani F, Consolini L, Thome JR. Experimental study on condensation heat transfer in vertical minichannels for new refrigerant R1234ze(E) versus R134a and R236fa. Exp Therm Fluid Sci 2011;35:442–454. DOI: 10.1016/j.expthermflusci.2010.11.006

[21] Kim S-M, Mudawar I. Universal approach to predicting heat transfer coefficient for condensing mini/micro-channel flow. Int J Heat Mass Tran 2013;56:238–250. DOI: 10.1016/j.ijheatmasstransfer.2012.09.032

[22] Mikielewicz D, Wajs J. Possibilities of heat transfer augmentation in heat exchangers with minichannels for marine applications. Pol Marit Res 2017;24(S1):133–140. DOI: 10.1515/pomr-2017-0031

[23] Wajs J, Mikielewicz D, Fornalik-Wajs E, Bajor M. Recuperator with microjet technology as a proposal for heat recovery from low-temperature sources. Archives of Thermodynamics 2015; 36(4):48–63. DOI: 10.1515/aoter-2015-0032

[24] National Institute of Standards (NIST). Refprop v. 9.0; 2010.

[25] F-Chart Software. Engineering Equation Solver (EES); 2012.

[26] Mikielewicz J. Semi-empirical method of determining the heat transfer coefficient for subcooled saturated boiling in a channel. Int J Heat Mass Tran 1973;17(10):1129–1134.

[27] Müller-Steinhagen R, Heck K. A simple friction pressure drop correlation for two-phase flow in pipes. Chem Eng Prog 1986;20:297–308.

[28] Kandlikar SG. Scale effect on flow boiling heat transfer in microchannels: A fundamental perspective. Int J Therm Sci 2010;49(7):1073–1085. DOI: 10.1016/j.ijthermalsci.2009.12.016

[29] Zivi SM. Estimation of steady state steam void fraction by means of the principle of minimum entropy production. J Heat Trans-T ASME 1964;86(2):247–251.

[30] Suryanarayana N.V. Forced Convection – External Flows, chapter 3.2.2. In: Kreith F, editor. The CRC Handbook of Thermal Engineering, Boca Raton: CRC Press LLC; 2000.

[31] Peters MS, Timmerhaus KD, West RE. Plant design and economics for chemical engineers. New York: McGraw-Hill; 2003.

[32] Kapale UC, Chand S. Modeling for shell-side pressure drop for liquid flow in shell-and-tube heat exchanger. Int J Heat Mass Tran 2006;49(3-4):601–610. DOI: 10.1016/j.ijheatmasstransfer.2005.08.022

[33] Office of Technical Inspection. UDT-UC/2005, Specifications for pressure equipment; 2005 (in polish).

[34] Mukherjee R. Effectively design shell-and-tube heat exchangers. Chem Eng Prog 1998;94(2):21–37.

[35] Kosowski K, Piwowarski M, Stępień R, Włodarski W. Design and investigations of the ethanol microturbine. Archives of Thermodynamics 2018; DOI: 10.1515/aoter-2018-0011

HIGHLIGHTS:

- Shell-and-tube condenser with minichannels is considered.
- Sizing calculations of condenser dedicated to micro-CHP ORC unit are performed.
- In-house model of pressure drop and condensation is applied to heat exchanger sizing.
- Experimental validation of the prototype shell-and-tube heat exchanger is carried out.